Measurement of Absolute Water Density, 1 °C to 40 °C

Measurement of Absolute Water Density, 1 °C to 40 °C

J. B. Patterson and E. C. Morris

Abstract. The absolute density of Standard Mean Ocean Water (SMOW) has been determined over the range 1 °C to 40 °C by weighing a hollow sphere of known volume in air-free water samples of measured isotopic content. The volume of the sphere as a function of temperature is known as a result of a combination of interferometric and mechanical measurements. The measured densities are tabulated. A formula (as proposed by Thiesen et al. [14]) and a fifth-order polynomial in temperature have been fitted to the tabulated data by least-squares analysis. The density calculated from the polynomial is estimated to have a standard uncertainty ranging from 0,64 parts in 10^6 at 15 °C to 1,4 parts in 10^6 at 1 °C and 40 °C. Comparisons are made with published data.

1. Introduction

Pure air-free water of known isotopic content is a very convenient standard of density. Due to doubt concerning the accuracy of the present water density tables, which still rely heavily on data obtained at the beginning of the twentieth century [1], standards laboratories have undertaken to remeasure water density using several methods. At the CSIRO National Measurement Laboratory (NML), a sphere of known volume is weighed in air-free water of known isotopic content. Two preliminary reports of the early work carried out at the NML have already been published [2, 3], and dilatation equations have been proposed, together with a tentative value for the absolute density of Standard Mean Ocean Water (SMOW) at 4 °C.

Recent examination of the mass and diameter measurements for the glass sphere made in the early NML work indicates that systematic errors are likely. It is also possible that some of the data upon which the provisional results [3] were based are not for air-free samples. Below, it is shown how these errors have been eliminated, and the apparatus and method are described in greater detail than before. Improvements made since the earlier reports are discussed.

2. Principle of the Measurement

To measure the density of water, the mass of water displaced by an object of accurately known volume is measured. In the present project the density measurements extend from 1 °C to 40 °C, so the volume of the immersed object must be a known function of temperature over this range.

Cubic objects have sometimes been chosen for density work, but an evacuated hollow glass sphere made from an ultra-low expansion (ULE) glass [3] was used in this case. The spherical form was chosen because it is relatively easy to manufacture and is less susceptible to damage than a cube with sharp edges. The sphere was made hollow so that its apparent mass when weighed in water is small and can be measured with a relatively sensitive balance.

This method of measurement is critically dependent on the quality of the sphere and the measurement of its volume. The present sphere has a diameter of approximately 76 mm and consists of two hemispheres glued together, the glue line being referred to here as the "equator". Along the equator, light scattering in the glue eliminates reflections originating at the inside surfaces and allows accurate diameter measurements at five equally spaced points (i.e. every 36°) with a Saunders interferometer [4, 5]. These points are located to within ± 1 mm using a scale drawn on the inside surface of the sphere.

To complete the absolute measurement of the sphere volume at 20 °C, a Talyrond roundness machine was used to measure the relative diameter at eighteen equally spaced points (i.e. every 10°) along the five meridians which cross the equator at the points where the diameter had been measured interferometrically. The first Talyrond measurement on each meridian was at this equatorial point. A total of 648 Talyrond measurements was made and they indicate a maximum variation in the diameter of the sphere of 195 nm.

The variation of sphere volume with temperature was calculated from interferometric measurements at a number of points along the equator and along one

J. B. Patterson and E. C. Morris: CSIRO Division of Applied Physics, PO Box 218, Lindfield, NSW 2070, Australia.

meridian. This work extended from 7 °C to 40 °C, and the extrapolation of the resulting relationship to 1 °C introduces an additional uncertainty which is most significant at 4 °C, where it accounts for about 20 % of the total uncertainty of the measured water density. For the meridional measurements, unwanted reflections from the inside surfaces were eliminated by an aluminium strip evaporated on to the sphere along the meridian.

The apparent mass of the sphere in air was measured, and the true mass calculated by careful measurement of the air density at the time of the weighing. The apparent mass of the sphere in the water sample was measured by mounting the sphere on a carrier, submerging it, and measuring the change in the mass recorded by the balance when the sphere was lifted off the carrier by a mechanical device.

The upthrust on the sphere was calculated from these two mass values and, using the principle of Archimedes, the density of the water was determined, knowing the volume of the liquid displaced by the sphere.

The water sample in which the sphere was weighed, was maintained, throughout the weighings, at a temperature (t) close to specified nominal temperatures (t_n) within the range 1 °C to 40 °C. The density $\rho(t, P)$ of water at temperature t and pressure P was derived from the equation

$$\rho(t, P) = [M_a - M_w(1 - \sigma/\rho_m)(g_m/g_s)]/V(t), \quad (1)$$

where

t is the water temperature during the apparent mass measurement,

P is the pressure in the water during the apparent mass measurement,

M_a is the true mass of the sphere,

M_w is the apparent mass of the sphere in water at temperature t and pressure P, i.e. the combined mass of the standards which balance the sphere in water,

σ is the air density during the apparent mass measurement,

ρ_m is the density of the mass standards used for measuring M_w,

g_m is the gravitational acceleration at the level of the mass standards used for measuring M_w,

g_s is the gravitational acceleration at the sphere level,

$V(t)$ is the volume of the sphere at temperature t.

3. Apparatus

A schematic diagram of the apparatus for determining the apparent mass of the sphere in the water samples is shown in Figure 1. The balance is situated above the temperature-controlled bath on a stable platform

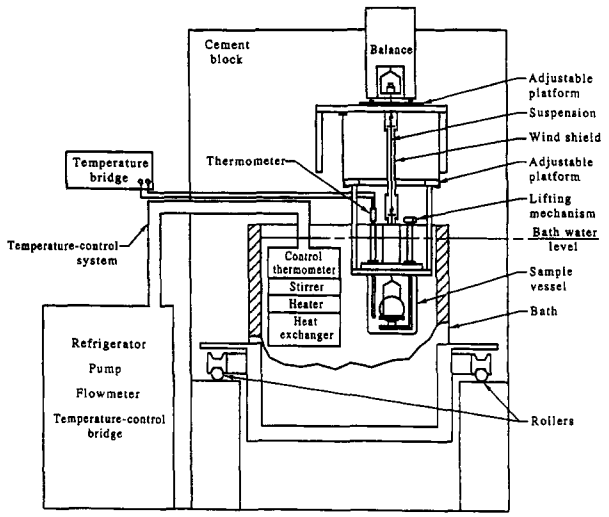

Figure 1. Schematic diagram of the apparatus for weighing in water.

attached to a large cement pillar in order to minimize vibration.

The bath can be rolled forward on rails from underneath the balance to allow the sample vessel holding the water to be lifted in and out of the bath. The temperature of the bath can be set to, and controlled at, any temperature between 1 °C and 40 °C. The accuracy of control (both spatial and temporal) is such that the temperature is observed to vary within a range of 0,005 °C. Within the water sample itself, however, no significant temperature variations were observed.

3.1 Sample vessel

A vessel was designed to hold the water sample in such a way that the exposure to air is minimal, and the sphere can be lifted on and off the suspended carrier with a mechanical lifting device. A diagram of the vessel is shown in Figure 2. The stainless steel lid slopes on the underside so that air bubbles are not trapped when the vessel is filled with water.

The glass sight tube above the lid is sealed on the outside so as to prevent entry of water from the bath and has a constricted neck, a few millimetres internal diameter, at the lower end to restrict the passage of dissolved air into the main body of the water sample. The vessel is filled with the sample of water to a level just below an open glass side tube, set at an angle, through which a small drop of detergent can be added to the water surface to stabilize surface tension. The detergent was used in the later work (samples 7 to 10) but not in the early work (samples 1 to 6): since the mean measured SMOW density at 4 °C is the same for both, to within 0,15 parts in 10^6, the detergent does not seem to have affected the density of the water sample below the constricted section.

The two tubes through the lid, holding the thermometer and the lifting rod, are also sealed from

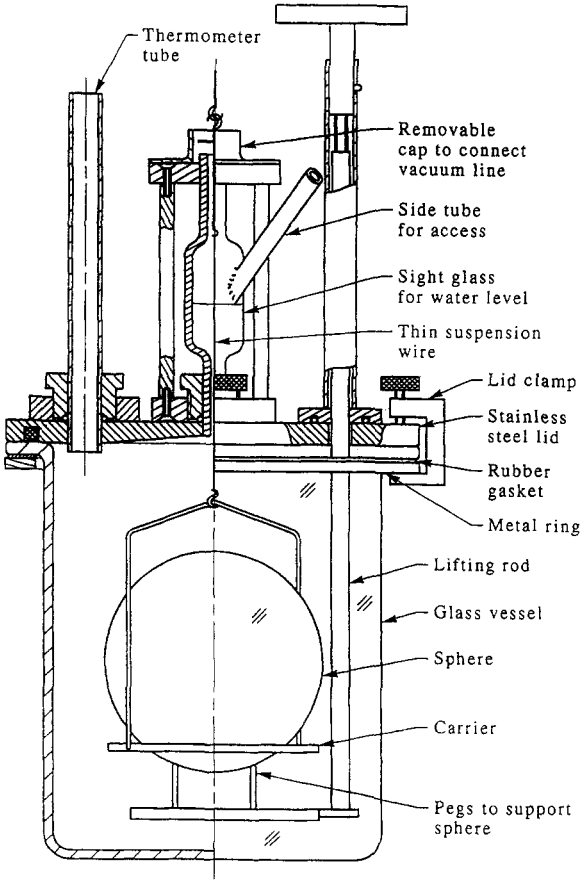

Figure 2. Diagram of the sample vessel.

the bath on the outside, and are of diameters such that only a small area of water is exposed to the air.

The sample vessel is suspended from a platform held below the balance. A facility, on both the balance and vessel platforms, allows alignment of the centre lines of each system. The suspension rod, attached to the bottom of the balance pan, takes the form of four separate sections which can be hooked together to hold the carrier which holds the sphere inside the vessel. The suspension is made of stainless steel and the section passing through the water surface is a wire, 0,08 mm diameter, which reduces the effect of surface tension to a minimum. A wind shield is provided to prevent air disturbance of the suspension system.

A system comprising a lifting rod and platform is used to load and unload the sphere from the carrier. When this loads or unloads the sphere from the carrier, it is necessary to adjust the water level back to the original position, using the thermometer (see below) as a displacement rod. The water level in the sight tube is monitored by the cross hairs of a telescope, positioned in front of the bath observation window.

The carrier holding the sphere hangs symmetrically, and is aligned so that the suspension system remains vertical when the sphere is loaded and unloaded. This prevents the suspension wire from interfering with the narrow-necked section of the sight tube.

For accurate temperature measurement, the resistance of a calibrated platinum resistance thermometer, held level with the centre of the sphere, is measured with a resistance bridge. The maximum thermometer movement required to adjust the water level is less than 15 mm, a distance over which the temperature gradient is negligible. The water pressure in the horizontal plane passing through the centre of the sphere is found by adding the air pressure (measured with an aneroid barometer) to the head of water above the plane.

3.2 Balances used for hydrostatic weighing

The modified Mettler H51 balance used in earlier work [3] has been replaced by a Sartorius Mass Comparator Model No. 2086, adjusted to a resolution of 0,01 mg. The new balance requires fewer calibrated masses and has a computer interface. In other important respects (absolute accuracy, for example) it is very similar to the Mettler.

An advantage of this balance is that it is a null reading device so that the position of the suspension system is the same for all readings taken. This ensures that the water surface cuts the thin suspension wire at the same position for all readings, after adjustment of the water level for the change in loading conditions of the carrier. (For the modified Mettler balance, the movement of the suspension was also very small: approximately 0,03 mm.)

The apparent mass of the sphere in the water sample is determined by comparing it with standard masses placed on the balance pan and reading the mass difference on the balance read-out. It is preferable to manipulate the masses with the balance case closed, so a special stainless steel mass of 100 grams was made in the shape of a pan so that it could be lifted on and off the normal balance pan by a lever operated from outside the balance case. The smaller masses required to make up the correct mass value to within 0,01 grams are placed on this removable pan.

3.3 Saunders interferometer and Talyrond roundness measuring instrument

The Saunders interferometer [4] is shown in Figure 3. The sphere and etalon are housed in a temperature-controlled box and the laser beams are directed through open windows so as to reflect off the etalon and sphere surfaces. A calibrated probe within the box measures relative humidity, and the air temperature is measured by thermocouples attached to the inside surface of the etalon. The air pressure is measured by an aneroid barometer.

The sphere is supported on a cone-shaped base attached to a vertical centre rod, which can be rotated through 180° without moving the sphere appreciably off-axis. A scale drawn on the inside surface of the sphere allows the operator to keep track of its orientation to within ± 1 mm along the circumference.

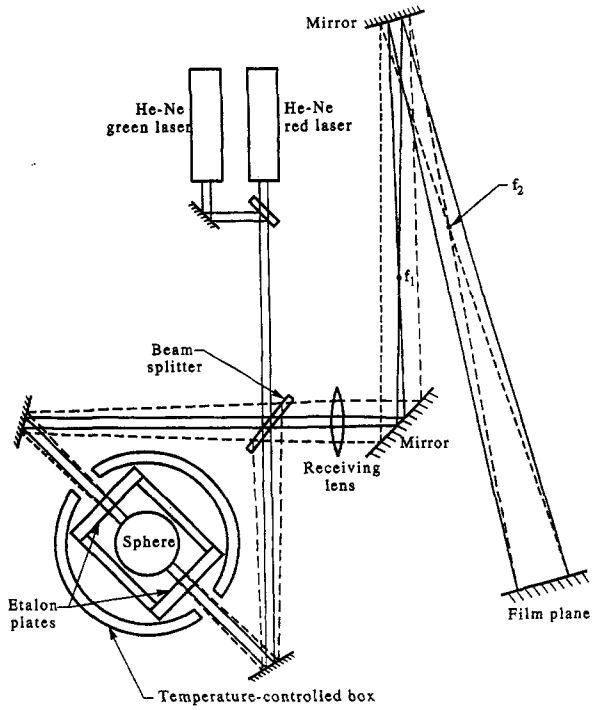

Figure 3. Diagram of the Saunders interferometer.

The mechanical design also allows the sphere to be lowered away from the beams to align the etalon.

For the present work, the etalon used previously [3] was replaced by one lent to the NML by the National Research Laboratory of Metrology (NRLM) of Japan. This etalon consists of two plates optically contacted to a cylindrical spacer which has a large hole in the side to allow the sphere to be raised into or lowered from the etalon. The entire etalon is made of fused quartz.

The Rank Taylor Hobson model 73 Talyrond roundness machine can be used to measure variations in radius along any great circle of the sphere. In this work, recent improvements in the technique of roundness measurement [6] were implemented.

4. Procedure

4.1 Mass of the sphere

A review of the mass determinations for the sphere has cast doubt on the earlier measurements reported in [2]. Not only have some of the associated air density readings been found to be unreliable, but there is also a source of error linked to the cleaning of the sphere. As can be seen from measurements made in 1992 and summarized in Figure 4, the mass of the sphere does not stabilize for several days after cleaning.

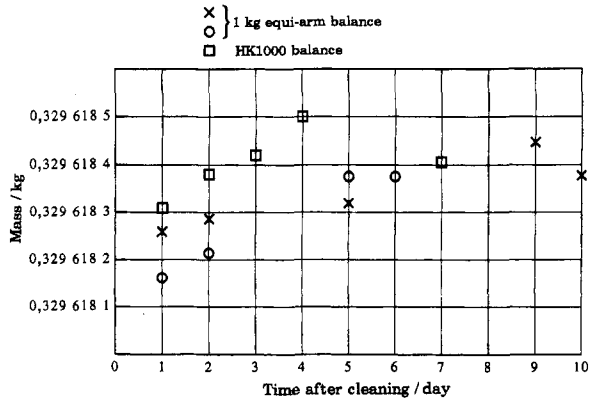

Figure 4. Summary of the mass-in-air readings for the sphere after cleaning (X and O indicate two separate weighing runs).

The mass adopted for the sphere was therefore derived from 1992 measurements made at least four days after cleaning. These measurements consist of two sets on different balances (see Table 1 and Figure 4), for both of which the air density required for the buoyancy correction was calculated from temperature, pressure and humidity measurements, using the CIPM-81 equation [7]. (For this purpose, the difference between the CIPM-81 equation and the more recent 1981/91 equation [8] is negligible.)

The eighty-eight readings were combined to give an overall mean mass value of 0,329 618 411 kg with a standard deviation of 0,000 000 040 kg. A check was made to measure the effect of static charge (if any) on the sphere surface by using a radioactive source inside the case of the HK1000MC for several sets of readings. No significant change in mass reading was detected with the source present.

4.2 Volume of the sphere

The volume was calculated from ninety diameter measurements made along five meridians. The equatorial diameter on each meridian was measured in the Saunders interferometer. The other diameters were found from Talyrond measurements giving the relative diameters at eighteen equally spaced points along each meridian, including the equatorial point.

The etalon and air-gap distances were measured under atmospheric conditions, and not in an evacuated chamber as in the early work. Changes in the laser wavelength were allowed for by using the revised version of Edlén's formula [9] in conjunction with measurements of the temperature, pressure and humidity of the air. An amendment to this formula [10]

Table 1. Measurements of the mass of the ULE sphere.

Set	Balance used	Number of readings	Mean mass/kg	Standard deviation of mean/kg
1	1 kg Oertling	50	0,329 618 379	0,000 000 042
2	HK1000MC	38	0,329 618 452	0,000 000 044

does not change the wavelength by more than 0,01 parts in 10^6.

As a further change to the earlier work, two lasers of different wavelength were used. Two factors, taken together, make it very unlikely that any error was incurred in determining the integral orders. First, the 648 Talyrond measurements referred to in Section 2 show that the diameter variation along the equator is unlikely to exceed 120 nm, and this is consistent with the results of the exact fractions analysis using the two lasers, which showed a variation of up to 95 nm; second, a consistent error in the integral order of the diameters would be obvious from the values of water density obtained. It would not matter whether this error was associated with the etalon or with the gap measurements.

The thickness and phase correction measurements associated with the aluminium-coated spots at each end of the measured diameters were sources of considerable uncertainty in the early NML work [3]. However, as discussed in Section 2, the use of coatings can be avoided if the diameters are located along the equator, where the glue line eliminates unwanted reflections from the inner surface of the sphere.

4.2.1 Etalon measurement

A calibrated stabilized He-Ne red laser was used as the main light source, and a He-Ne green laser, modified to produce a stable wavelength, was used as a second light source. The two laser beams were directed, in turn, through the etalon at a small divergent angle, using a combination of two lenses, so as to produce Haidinger rings at the focal point of the receiving lens (see Figure 3). The rings were photographed and their diameters measured using a profile projector in association with a coordinate table. Six rings were measured for each photograph, and the fringe fraction at the centre of the pattern was obtained by linear regression [4].

Having established the integral order at 20 °C by an exact fractions analysis, the He-Ne red laser alone was used to measure the etalon length at other temperatures (see Section 4.2.3). The etalon length was fitted to a quadratic in temperature which is in good agreement with several measurements for the same etalon made at the NRLM between 1977 and 1989 [11].

4.2.2 Air-gap measurement

Both lasers were used in a single set of measurements at 21 °C. This set consists of five photographs for the He-Ne red laser and two for the He-Ne green laser, taken alternately from each side of the sphere, at each diameter position, so as to eliminate any error due to the sphere and etalon moving relative to one another during the measurement. The He-Ne green photographs were used only to determine the integral order of fringes in the total air gap. Having established the integral orders, the red laser alone was used at other temperatures.

The fringe fraction at the centre of the ring pattern was determined by linear regression as in Section 4.2.1. For each set of measurements, the five fringe fraction values obtained by the He-Ne red laser were used to calculate the mean fringe fraction E_m of the total air gap. The value of this gap calculated from E_m, the integral order, and the corrected wavelength, was subtracted from the etalon distance to obtain the diameter of the sphere.

4.2.3 Temperature dependence of the sphere diameter

In order that the volume of the sphere be known over the full temperature range of interest, the etalon calibration and the air-gap measurements were carried out at temperatures from 10 °C to 40 °C (etalon) and 7 °C to 40 °C (gap) by controlling the temperature of the box surrounding the sphere and etalon. (Heat leaks in the present apparatus make it impossible to extend these measurements to 1 °C.)

The temperature was measured using three equally spaced thermocouples attached to the etalon spacer; the thermocouples were referenced to a platinum resistance thermometer located nearby in the temperature-controlled region. The average of the thermocouple readings was used to calculate the temperature of the length measurement. The temperature variations indicated by the thermocouples were usually quite small, but became significant at the higher temperatures reaching a maximum of 0,25 °C (standard deviation) at 40 °C.

Most of the gap measurements were for equatorial diameters, but to check for the possibility that the sphere expansion might not be isotropic, measurements were also carried out at five equally spaced points arround a narrow aluminium strip evaporated on to the sphere along a meridian. These meridional data were used in the derivation of (2) below, but not for the determination of the absolute sphere volume.

The common least-squares solution for the diameter/temperature relationship obtained using all the data was

$$d(t) = d_0 [1 - 6,408 \times 10^{-8}\, t/°\mathrm{C} + 9,785 \times 10^{-10}\, (t/°\mathrm{C})^2], \quad (2)$$

where

$d(t)$ is the mean sphere diameter at temperature t,
d_0 is the mean sphere diameter at temperature 0 °C.

In Figures 5 and 6, the various sets of diameter measurements are compared with (2), and it can be seen that there is no significant anisotropy.

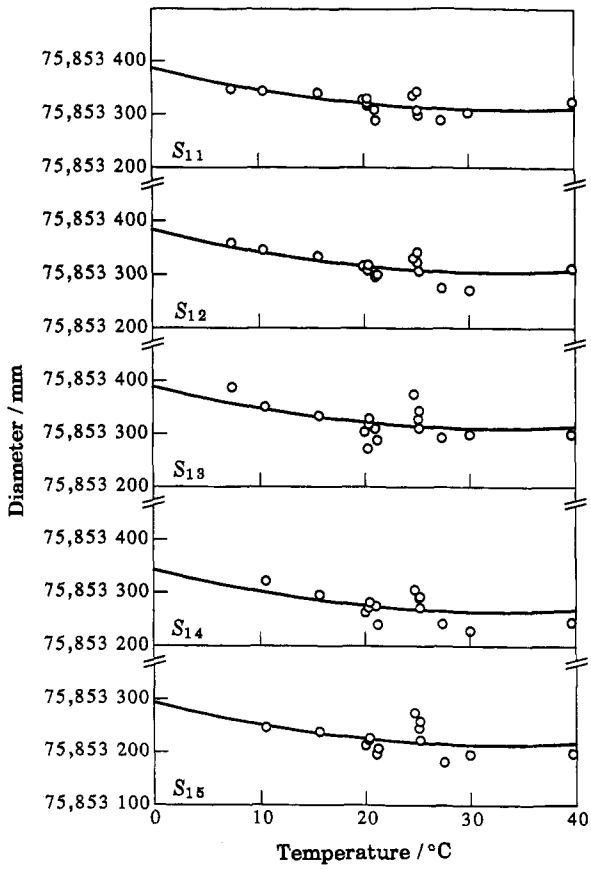

Figure 5. Dilatation of the sphere diameter around the equator. The identification codes S_{jk} have the following meaning: k is the number used to identify each of the five meridians, while j identifies each of the five equally spaced positions along the meridians starting with $j = 1$ for the equator.

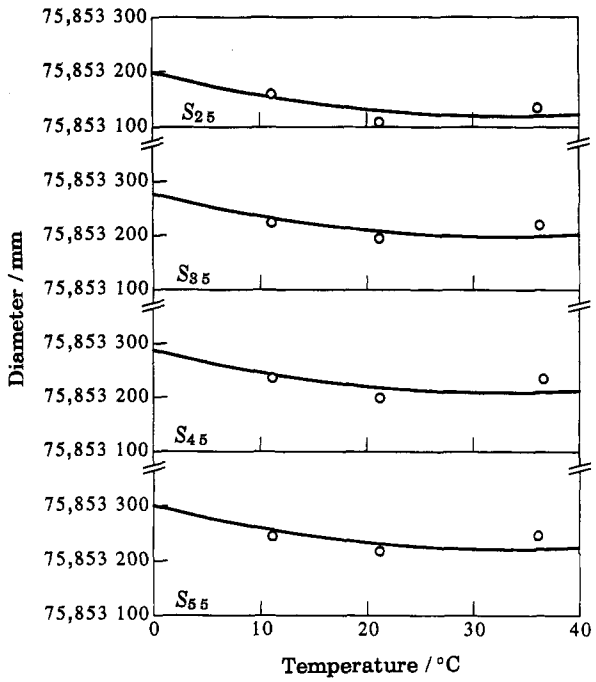

Figure 6. Dilatation of the sphere diameter along a meridian. The identification codes S_{jk} have the following meaning: k is the number used to identify each of the five meridians, while j identifies each of the five equally spaced positions along the meridians starting with $j = 1$ for the equator.

4.2.4 Relative diameter measurements with a Talyrond machine

The variations in radius along five meridians were measured at 20 °C. These meridians pass through the five points on the equator for which the diameter had already been measured by interferometry. A total of thirty-six equally spaced points along each meridian was chosen. Data from opposing points were combined to give eighteen relative diameter measurements, one of which corresponded to the equatorial diameter measured by interferometry.

4.2.5 Calculation of sphere volume

The volume of the sphere at 20 °C was calculated by combining the five equatorial diameters obtained by interferometry at 20 °C with the Talyrond measurements along the meridians. The total volume of the sphere at 20 °C is thus

$$V(20) = \frac{1}{24} \sum_{i=1}^{5} \sum_{j=1}^{18} \omega_{ij} (d_i + S_{ij})^3, \qquad (3)$$

where

d_i is the ith equatorial diameter. The point on the equator where it is measured defines the ith meridian.

S_{ij} is $s_{ij} - s_{i1}$.

s_{ij} is the jth relative diameter on the ith meridian. Its position in degrees is $10(j - 1)$ along the meridian from the equator.

ω_{ij} is the solid angle associated with s_{ij}.

Except for the five polar points ($j = 10$, $i = 1$ to 5), each s_{ij} refers to a unique diameter. The solid angle ω_{ij} ($j \neq 10$) is defined by the areas (at both ends of the diameter) which extend half way in both latitude and longitude from the point (i, j) to the adjacent points. For the polar points ω_{ij} is $9{,}564 \times 10^{-3}$ sr, one-fifth of the solid angle occupied by a double-ended cone having a half-angle at the vertex of $\pi/36$ rad (5°).

The volume at 20 °C calculated from (3) is 228,518 412 cm^3 and the corresponding mean diameter is 75,853 250 mm. Using (2), the volume as a function of temperature is

$$V(t) = 228{,}519\,022\,[1 - 1{,}922 \times 10^{-7}\, t/°\mathrm{C} + 2{,}936 \times 10^{-9}\, (t/°\mathrm{C})^2], \qquad (4)$$

4.3 Water sample preparation

The water samples were taken from distilled water storage vessels, and in most cases were distilled again in a glass still. In the early NML work, the procedure for de-aerating the samples was to fill the sample vessel

partially with the water, insert the sphere and carrier, and seal the lid. The space left above the water surface was evacuated while heating the vessel to a temperature of 40 °C for a period of at least 30 minutes. The vessel was then topped up with a boiled sample from the same source, and the thermometer inserted to restrict the surface area of water exposed to air.

In the later NML work, the distilled samples were boiled for at least 30 minutes in a vessel which could be isolated from the air after the boiling was stopped. After cooling to a temperature of about 60 °C, the sample was poured into the sample vessel, the sphere inserted and the lid sealed as quickly as possible. The sample was then ready to be cooled to lower temperatures for the measurements.

Measurement of the isotopic ratios O_{18}/O_{16} (R_{18}) and D/H (R_d) of the water samples was carried out by the Institute of Nuclear Sciences, DSIR, New Zealand (samples 2 to 5), the Australian Atomic Energy Commision (sample 6), and the Division of Water Resources, CSIRO, Australia (samples 7 to 10). The ratios were not measured for sample 1 as data for this sample were not used to establish the absolute density (see Section 5). The correction required to convert the measured density of a water sample to the corresponding value for Vienna Standard Mean Ocean Water (V-SMOW), was calculated from [12]:

$$\rho_{\text{sample}} - \rho_{\text{SMOW}} = (0,233\,\delta_{18} + 0,016\,6\,\delta_d)\ \text{kg/m}^3, \quad (5)$$

where

$$\delta_{18} = [R_{18}/(2\,005{,}2 \times 10^{-6})] - 1,$$

and

$$\delta_d = [R_d/(155{,}76 \times 10^{-6})] - 1.$$

The ratios and the corresponding correction for each sample are shown in Table 2.

Table 2. Isotope ratios of the water samples, and the resulting correction to V-SMOW.

Sample number	$R_{18} \times 10^6$	$R_d \times 10^6$	Correction (kg/m^3)
2	1 982,4	144,8	+0,003 82
3	1 985,6	146,0	+0,003 32
4	1 990,4	149,0	+0,002 40
5	1 990,4	149,0	+0,002 40
6	1 999,9	153,0	+0,000 91
7	1 989,5	147,6	+0,002 69
8	1 989,6	147,5	+0,002 70
9	1 985,7	146,2	+0,003 29
10	1 983,9	145,6	+0,003 56

4.4 Water weighings

The special vessel was attached to a platform in the temperature-controlled bath and its position was adjusted to align the interconnecting suspensions between the balance and the sphere carrier. The length of one of the suspension rods was adjustable to leave the clearance between the sphere and carrier as small as possible. This precaution prevented undue disturbance to the water between weighings. Care was taken that there was no interference on the suspension system at any time during the weighings.

A full description of the weighing system used on the Mettler H51 balance is given in [3], and is not repeated here. The Sartorius comparator compared the apparent mass M_w of the sphere in water with the mass M_0 of a counterweight in air. The mass M_0 was equal to M_w to within 0,01 grams, and M_w was found from the equation

$$M_w = M_0 + [R_2 - (R_3 + R_1)/2], \quad (6)$$

where R_1, R_2 and R_3 are successive readings of the balance. For R_1 and R_3, the counterweight was present on the balance pan and the sphere was unloaded from the carrier. For R_2, the counterweight was unloaded and the sphere was loaded on to the carrier. This set of weighings was repeated several times and the air temperature, pressure and humidity were recorded after every third set.

5. Results

Measurements of the apparent mass M_w of ten samples of water are reported here and Tables 3 to 12 show the data in the order of acquisition. The third column of each table shows the number of M_w measurements at each temperature, while the fourth column shows the mean density obtained from them. The densities have been adjusted to the nominal temperature shown in the second column and to standard atmospheric pressure (101 325 Pa) using the compressibility and thermal expansion data of Kell [13]. The temperature of the density measurements was always within ±0,02 °C of the nominal temperature, and the pressure was within ±3 000 Pa of the standard atmosphere.

For all samples except the first, the tabulated densities have also been adjusted to V-SMOW using (5) and the isotope ratios shown in Table 2. The last column in Tables 3 to 12 lists the ratio ρ/ρ (4), where ρ is the density in the fourth column and ρ (4) is the mean measured value of ρ at 4 °C for the given water sample.

Samples 1 to 6 form the basis of the provisional results already published [3]. The present treatment of these samples differs from that of the earlier analysis in three ways: (a) a new value has been adopted for the mass of the sphere due to inadequacies in the early data (see Section 4.1); (b) a new formula for the volume of the sphere has likewise been used (see Sections 4.2 and 4.2.5); and (c) the temperatures have been adjusted from the IPTS-68 to the ITS-90.

Table 3. Density and dilatation values for sample 1.

Date	Temperature/°C	Number of measurements	Mean density/ (kg/m³)	ρ/ρ (4)
1979-07-26	4	9	999,964 83	
1979-07-27	1	9	999,891 68	0,999 927 01
1979-07-27	4	6	999,964 90	
1979-07-31	4	9	999,964 62	
1979-08-01	2	9	999,933 14	0,999 968 47
1979-08-01	3	9	999,957 14	0,999 992 47
1979-08-01	4	6	999,964 60	
1979-08-02	5	9	999,956 71	0,999 992 04
1979-08-02	6	8	999,932 78	0,999 968 11
1979-08-03	7	9	999,894 26	0,999 929 59
1979-08-03	4	6	999,964 41	

Table 4. Density and dilatation values for sample 2.

Date	Temperature/°C	Number of measurements	Mean V-SMOW density/ (kg/m³)	ρ/ρ (4)
1980-05-20	4	12	999,973 27	
1980-05-21	10	6	999,700 79	0,999 727 51
1980-05-22	15	6	999,100 75	0,999 127 45
1980-05-23	20	6	998,206 91	0,998 233 59
1980-05-28	25	9	997,044 90	0,997 071 54

Table 5. Density and dilatation values for sample 3.

Date	Temperature/°C	Number of measurements	Mean V-SMOW density/ (kg/m³)	ρ/ρ (4)
1980-07-07	4	12	999,973 49	
1980-07-08	10	9	999,702 15	0,999 728 65
1980-07-09	15	9	999,103 36	0,999 129 84
1980-07-10	20	9	998,207 17	0,998 233 63
1980-07-13	25	9	997,047 05	0,997 073 47
1980-07-14	30	9	995,644 78	0,995 671 16

Table 6. Density and dilatation values for sample 4.

Date	Temperature/°C	Number of measurements	Mean V-SMOW density/ (kg/m³)	ρ/ρ (4)
1980-08-06	4	12	999,972 86	
1980-08-07	20	9	998,204 86	0,998 231 95
1980-08-08	40	11	992,212 49	0,992 239 40

Table 7. Density and dilatation values for sample 5.

Date	Temperature/°C	Number of measurements	Mean V-SMOW density/ (kg/m³)	ρ/ρ (4)
1980-10-22	4	9	999,974 33	
1980-10-23	20	9	998,207 03	0,998 232 65
1980-10-24	40	9	992,215 16	0,992 240 61

Table 8. Density and dilatation values for sample 6.

Date	Temperature/°C	Number of measurements	Mean V-SMOW density/ (kg/m³)	ρ/ρ (4)
1980-06-03	4	9	999,974 44	
1980-06-04	10	9	999,701 99	0,999 727 54
1980-06-05	15	9	999,101 51	0,999 127 05
1980-06-06	20	9	998,204 09	0,998 229 60
1980-06-07	25	10	997,046 87	0,997 072 35
1980-06-08	30	9	995,645 56	0,995 671 00

Table 9. Density and dilatation values for sample 7.

Date	Temperature/°C	Number of measurements	Mean V-SMOW density/ (kg/m³)	ρ/ρ (4)
1990-09-05	4	11	999,973 44	
1990-09-05	4	11	999,973 45	
1990-09-06	4	12	999,973 37	
1990-09-07	4	11	999,973 36	
1990-09-10	4	10	999,973 47	
1990-09-11	10	12	999,700 92	0,999 727 23
1990-09-11	15	12	999,100 88	0,999 127 18
1990-09-11	20	12	998,204 71	0,998 230 98
1990-09-12	25	10	997,045 23	0,997 071 46
1990-09-12	25	5	997,046 85	0,997 073 08
1990-09-12	30	11	995,649 13	0,995 675 32
1990-09-13	40	12	992,215 33	0,992 241 43
1990-09-17	20	9	998,206 32	0,998 232 59
1990-09-17	20	7	998,205 44	0,998 231 71
1990-09-18	4	9	999,973 75	
1990-09-18	4	6	999,974 28	

Table 10. Density and dilatation values for sample 8.

Date	Temperature/°C	Number of measurements	Mean V-SMOW density/ (kg/m³)	ρ/ρ (4)
1990-09-20	4	11	999,972 09	
1990-09-21	10	12	999,699 40	0,999 726 61
1990-09-21	15	12	999,100 00	0,999 127 19
1990-09-24	20	12	998,204 63	0,998 231 80
1990-09-24	25	12	997,044 91	0,997 072 04
1990-09-25	30	12	995,648 96	0,995 676 05
1990-09-25	35	12	994,033 09	0,992 060 13
1990-09-26	40	12	992,214 63	0,998 241 62
1990-09-27	4	12	999,972 90	
1990-09-27	2	9	999,940 91	0,999 968 13
1990-09-28	3	6	999,965 26	0,999 992 48
1990-09-28	3,5	6	999,971 15	0,999 998 37
1990-09-28	3,75	12	999,972 67	0,999 999 89
1990-10-03	4	6	999,973 34	
1990-10-03	4,25	12	999,972 85	1,000 000 07
1990-10-04	4,5	6	999,971 43	0,999 998 65
1990-10-04	5	6	999,965 50	0,999 992 72
1990-10-05	6	9	999,941 61	0,999 968 83

Table 11. Density and dilatation values for sample 9.

Date	Temperature/°C	Number of measurements	Mean V-SMOW density/(kg/m³)	ρ/ρ (4)
1992-06-23	20	21	998,206 87	0,998 231 87
1992-06-24	10	15	999,702 57	0,999 727 61
1992-06-26	4	18	999,974 95	

Table 12. Density and dilatation values for sample 10.

Date	Temperature/°C	Number of measurements	Mean V-SMOW density/(kg/m³)	ρ/ρ (4)
1992-06-30	4	21	999,974 31	
1992-07-02	10	19	999,702 56	0,999 728 24
1992-07-03	20	18	998,207 22	0,998 232 86
1992-07-07	30	18	995,649 93	0,995 675 49
1992-07-08	40	18	992,215 78	0,992 241 24
1992-07-08	16	9	998,947 21	0,998 972 87
1992-07-08	16	9	998,947 30	0,998 972 96

The densities obtained for sample 1 were significantly lower (by about 6 parts in 10^6) than those of later samples, raising the possibility that the sample had been contaminated. Consequently, the sample 1 data were not used to establish the absolute density of water, but were included with the data used to determine the form of the density-temperature relationship. Sample 6 was specially prepared by the Australian Atomic Energy Commission, and contained a higher ratio of the heavier isotopes. The more recent data (samples 7 to 10) were obtained to check the possibility that the sphere mass and/or volume may have changed during the twelve years since samples 1 to 6 were measured.

Dilatation data are often represented by an equation proposed by Thiesen et al. [14]:

$$\rho/\rho_0 = 1 - \frac{A\,(t - t_0)^2\,(t + B)}{(t + C)}, \qquad (7)$$

where t is the temperature, and t_0 is the temperature at which water attains its maximum density ρ_0. Since t_0 is very close to 4 °C, ρ_0 differs from ρ (4) by less than 4 parts in 10^9 (see, for example, [13] and [14]). For this work ρ_0 and ρ (4) are thus effectively identical, so the dilatation data in Tables 3 to 12 were fitted directly to (7). The results were $t_0 = 3{,}981\,8$ °C, $A = 1{,}858 \times 10^{-6}$ (°C)$^{-1}$, $B = 316{,}338\,08$ °C and $C = 70{,}699\,73$ °C. To obtain the value of t_0, only the data for temperatures below 10 °C were considered; all the data were then used in a second fit to obtain the values for the other parameters.

The fifth-order polynomial

$$\rho/\rho_0 = 1 - [A\,(t - t_0) + B\,(t - t_0)^2 + C\,(t - t_0)^3 + D\,(t - t_0)^4 + E\,(t - t_0)^5] \qquad (8)$$

was also fitted to the dilatation data. Having put t_0 equal to the value obtained in the Thiesen fit, the other parameters were found using linear regression. The results were

$$t_0 = 3{,}981\,8\ °C$$

$$A = 7{,}013\,4 \times 10^{-8}\ (°C)^{-1}$$

$$B = 7{,}926\,504 \times 10^{-6}\ (°C)^{-2}$$

$$C = -7{,}575\,677 \times 10^{-8}\ (°C)^{-3}$$

$$D = 7{,}314\,894 \times 10^{-10}\ (°C)^{-4}$$

$$E = -3{,}596\,458 \times 10^{-12}\ (°C)^{-5}.$$

The Thiesen formula and the polynomial appear to represent the data equally well and give very similar figures for the sum of squares of residuals. However, the polynomial fit was chosen to represent the results of this work.

The second column of Table 13 shows the dilatation d (8) calculated from (8). The third column shows the difference between d (7) and d (8), where d (7) is the dilatation calculated from (7); i.e. it shows $[d(7) - d(8)] \times 10^6/d(8)$. The following two columns likewise compare other recent determinations of water dilatation with d (8): the fourth column shows the polynomial equation of Watanabe [15], while the fifth column shows the Thiesen equation of Takenaka and Masui [16]. The differences shown in columns four and five are also plotted in Figure 7.

Table 13. Comparison of the dilatation data presented here in (7) and (8) with those of Watanabe [15], and of Takenaka and Masui [16].

Temperature/°C	ρ/ρ_0 from (8)	10^6 × fractional difference from d (8)		
		(7)	[15]	[16]
1	0,999 927 7	−0,78	−1,04	−1,02
2	0,999 968 4	−0,36	−0,49	−0,44
3	0,999 992 4	−0,12	−0,16	−0,13
4	1,000 000 0	0,00	0,00	0,00
5	0,999 991 8	0,03	0,04	0,01
7	0,999 929 6	−0,04	−0,08	−0,14
10	0,999 728 1	−0,20	−0,39	−0,40
15	0,999 128 1	−0,17	−0,55	−0,31
20	0,998 232 1	0,09	−0,31	0,17
25	0,997 072 3	0,12	−0,30	0,41
30	0,995 674 3	−0,18	−0,75	0,19
35	0,994 058 5	−0,46	−1,19	−0,04
38	0,992 991 3	−0,36	−1,10	0,13
40	0,992 241 1	−0,11	−0,81	0,49

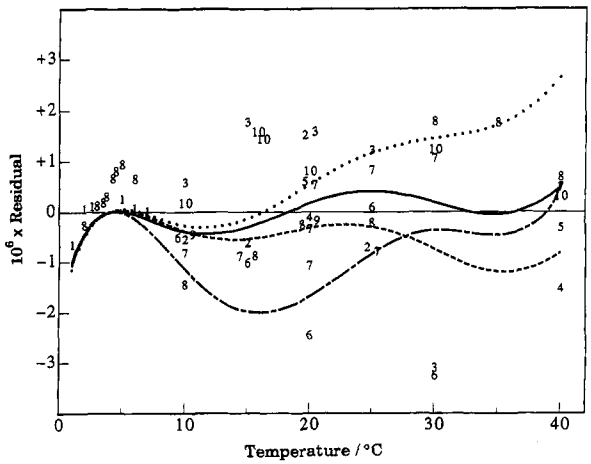

Figure 7. Residuals of the dilatation measurements relative to (8). Each residual is represented by its sample number. The curves represent the differences between the following data and (8):
- - - - - Watanabe [15]
——— Takenaka and Masui [16]
. . . . . Kell [18]
— — — — Bigg [17].

Figure 7 also shows curves representing the dilatation compilations of Bigg [17] and Kell [18]. These compilations are based on the work of Chappuis [19] and Thiesen et al. [14] whose data were related to the Echelle Normale (EN). It is assumed here that the EN is practically equivalent to the IPTS-68 [1], though Bigg and Kell assumed it to be equivalent to the IPTS-48; in Figure 7, the data of these authors have been adjusted to allow for this.

The Thiesen data (not shown in Figure 7) lie below the present results by up to 4 parts in 10^6 (near 40 °C), while the Chappuis data (also not shown) lie mostly above by up to 4,5 parts in 10^6 (at 40 °C).

In order to obtain a value of ρ_0 which, when substituted into (8), gives a formula which best represents the V-SMOW absolute density data for samples 2 to 10, these data were fitted to that equation with ρ_0 as the only adjustable parameter. The result is

$$\rho_0 = 999,973\,58\ \mathrm{kg/m^3} \tag{9}$$

Table 17 lists some densities calculated from (8) using this value for ρ_0 .

6. Uncertainty Estimation

The uncertainty associated with the absolute densities calculated from (8) and (9) is found from an estimation based on (1). All uncertainties are quoted at one standard deviation.

There are four significant contributions to the density uncertainty: the variances of the volume $V(t)$, of the true mass M_a, of the apparent mass M_w, and of systematic errors in the measurement of the water temperature t. There are also several small uncertainty contributions. The variances of random errors in the water temperature and pressure measurements are small and are accounted for as part of the apparent mass variance.

6.1 Volume variance

There are two contributions, $\mathrm{var_c}(d)$ and $\mathrm{var_u}(d)$, to the variance of the equatorial diameter measurements at 20 °C. The first of these arises from effects which are systematic for the five diameter measurements while the second is due to the five air-gap fringe-order measurements, which are not correlated. If $\mathrm{var}(s)$ is the variance associated with the s_{ij} in (3), then it follows from that equation that the variance of the volume V (20) is

$$\mathrm{var}(V_{20}) = \frac{\pi^2 d^4}{20}\,\mathrm{var_u}(d) + \frac{\pi^2 d^4}{4}\,\mathrm{var_c}(d) + \frac{5\,d^4\,\mathrm{var}(s)}{64} \times \left[\left(\sum_{j=2}^{18}\omega_{ij}\right)^2 + \sum_{j=2}^{18}\omega_{ij}^2\right], \tag{10}$$

where d is the mean diameter of the sphere.

The estimated contributions to $\mathrm{var_c}(d)$, $\mathrm{var_u}(d)$ and $\mathrm{var}(s)$ are listed in Table 14. These are mainly type A estimates, apart from $\mathrm{var}(s)$ which is known from studies of the technique and equipment used [6, 19]. From (10), $\mathrm{var}(V_{20})$ is found to be 0,002 6 $\mathrm{mm^6}$.

As well as these measurement uncertainties, there is a sampling uncertainty arising mainly from the choice of the five meridians. Using the 650 Talyrond measurements referred to in Section 2, this variance contribution was estimated to be 0,000 7 $\mathrm{mm^6}$; hence the total estimate for $\mathrm{var}(V_{20})$ is 0,003 3 $\mathrm{mm^6}$.

Table 14. Estimated variances associated with the measurement of sphere diameter at 20 °C.

Source	Variance of diameter/(nm)^2		
	Interferometer measurements		Mechanical measurement
	Systematic	Non-systematic	
Etalon calibration	7,6		
Air-gap fringe order		34	
Refractive index	12,6		
Laser wavelength	0,6		
Out-of-roundness measurement			22
Total	$\mathrm{var_c}(d) = 20,8$	$\mathrm{var_u}(d) = 34$	$\mathrm{var}(s) = 22$

The variance $\mathrm{var}(V)$ of $V(t)$ is found by adding to $\mathrm{var}(V_{20})$ the variance contribution associated with the experimentally determined term $V(t) - V(20)$. This contribution is estimated from the etalon and diameter linear regressions, together with an allowance

to account for spatial temperature variations observed in the interferometer between 30 °C and 40 °C (see Section 4.2.3); var (V) ranges from 0,003 3 mm^6 at 20 °C to 0,026 mm^6 at 40 °C and 0,061 mm^6 at 1 °C. The second column of Table 16 shows the density variance resulting from var (V).

6.2 Variances of mass measurements

The true mass of the sphere has been measured with an uncertainty of 40 μg, which corresponds to a water density uncertainty of 0,18 parts in 10^6. This is shown in the third column of Table 16 as a variance.

The systematic uncertainty in the measurement of M_w arises mainly from the calibration of standard masses and is estimated to be 0,1 parts in 10^6 in terms of the water density. The dispersion of the V-SMOW density data in Tables 4 to 12 is almost entirely due to the uncertainty in M_w arising from random effects. The density variance resulting from these effects has thus been estimated from the linear regressions used to obtain (8) and (9). The fourth column of Table 16 shows the total density uncertainty due to M_w uncertainty.

6.3 Variance due to systematic effects in water temperature measurement

The temperature near the sphere was measured with a platinum resistance thermometer with a calibration uncertainty of ± 2,5 mK. The corresponding variance in water density is listed in Table 16.

6.4 Small uncertainty contributions

There are several small contributions to the variance of the water density determination, which are listed in Table 15. The sum of these contributions is given in the sixth column of Table 16.

Table 15. Small contributions to the estimated water density variance.

Source	10^6 × relative standard deviation of source quantity	10^{12} × relative variance of water density
Air density measurement	800	0,003 2
Gravity ratio	< 0,01	< 0,000 1
Equating ρ_m to 8 000 kg/m^3 in (1)		0,001 6
Water pressure measurement	600	0,000 6
Isotopic ratios	100 for R_{18} 1 000 for R_d	0,002 5
Total		0,008 0

6.5 Total uncertainty of the water density determination

Table 16 shows the total estimated variance of the water density calculated from (8) and (9), together with the component variances; Table 17 shows the 1 σ uncertainty. There are approximately eighteen degrees of freedom associated with this estimate at 20 °C, and somewhat more at other temperatures. At 1 °C, the type A contributions make up almost 100 % of the total variance; they fall to 55 % at 15 °C, and at higher temperatures range between 35 % and 55 %.

7. Discussion

The experimental procedure employed at the NML for the measurement of absolute water density has been described, and several improvements made since the preliminary publication [3] have been mentioned. Rather than depend on separate dilatation measurements, the absolute density is measured throughout the range 1 °C to 40 °C. However, it is only at 20 °C that a complete measurement of the sphere volume is made; one can therefore expect that the uncertainty of the density measurement will be least near that temperature.

The greatest improvements that could be brought to the present method lie in the area of temperature

Table 16. Estimated relative variances associated with the water density calculated from (8) and (9).

Temperature/°C	10^{12} × variance of water density					
	Volume measurement	Mass in air	Apparent mass in water	Temperature measurement	Small contributions	Total
1	1,17	0,031	0,626	0,016	0,008	1,9
3	0,858	0,031	0,058	0,002	0,008	0,96
4	0,732	0,031	0,029	0,000	0,008	0,80
7	0,448	0,031	0,073	0,013	0,008	0,58
10	0,274	0,031	0,119	0,048	0,008	0,48
15	0,103	0,031	0,121	0,143	0,008	0,41
20	0,063	0,031	0,099	0,269	0,008	0,47
25	0,063	0,031	0,140	0,414	0,008	0,66
30	0,134	0,031	0,200	0,572	0,008	0,95
35	0,268	0,031	0,542	0,743	0,008	1,6
40	0,502	0,031	0,302	0,928	0,008	1,8

Table 17. SMOW densities calculated from (8) and (9), and their estimated uncertainties.

Temperature/°C	SMOW density (kg/m^3)	1 σ uncertainty (kg/m^3)
1	999,901 25	0,001 4
3	999,965 94	0,000 98
4	999,973 58	0,000 90
5	999,965 37	0,000 84
7	999,903 19	0,000 76
10	999,701 66	0,000 70
15	999,101 68	0,000 64
20	998,205 69	0,000 69
25	997,045 93	0,000 81
30	995,648 01	0,000 98
35	994,032 22	0,001 3
40	992,214 89	0,001 4

measurement and control. Without such improvements, there would be little point in reducing the 0,23 parts in 10^6 uncertainty with which the sphere volume at 20 °C was determined. At 40 °C, for example, the uncertainty could be halved by making large, but quite feasible, reductions in the temperature uncertainty. It is unlikely that the hydrostatic weighings could be upgraded very much.

It is unfortunate that temperature-control problems limited the measurement of sphere volume to 7 °C, though the resulting additional uncertainty at low temperatures is not great. If a new sphere were to be constructed by once again gluing together two hemispheres, the inner surface would be treated to eliminate reflections and allow interferometric diameter measurements at any point on its surface.

The present dilatation data are in good agreement with both recent determinations at the NRLM [15, 16]. In particular, the agreement with Takenaka and Masui is within 0,5 parts in 10^6 from 2 °C to 40 °C. Compilations carried out by Kell [18] and Bigg [17] differ from the results presented here by up to +2,6 parts in 10^6 and −2,0 parts in 10^6, respectively (see Figure 7). However, the data of Chappuis [19] and of Thiesen [14] diverge by up to +4,5 parts in 10^6 and −4,0 parts in 10^6, respectively.

The value reported here for the maximum density of V-SMOW is (999,973 58 ± 0,000 89) kg/m^3, at 3,982 °C. This is 0,001 42 kg/m^3, or 1,6 standard deviations less than the commonly accepted value of 999,975 kg/m^3 [1], which is based on measurements dating from the turn of the century.

Acknowledgements. Over the long period of this measurement, there are many people to thank for their contribution. The late Mr G. A. Bell, Mr A. L. Clarke and Dr E. G. Thwaite for the early work, Mr P. Neuweger and Mr A. Leistner for the manufacture of the sphere and other optical pieces and Mr P. Ciddor, Dr B. Ward and Dr N. Brown for their advice and work on the calibration and stability of the lasers. Mr W. Giardini must be thanked for the Talyrond measurements and Dr R. Masui and Dr K. Fujii of the NRLM for pointing out the errors involved in the original diameter measurements and for the loan of the etalon.

References

1. Menache M., Girard G., *Metrologia*, 1973, **9**, 62-68.
2. Bell G. A., Clarke A. L., *Atomic Masses and Fundamental Constants*, Vol. 5 (Edited by J. H. Sanders and A. H. Wapstra) New York, Plenum, 1976, 615.
3. Bell G. A., Patterson J. B., In *Precision Measurement and Fundamental Constants II* (Edited by B. N. Taylor and W. D. Phillips), Natl. Bur. Stand. (U.S.) Spec. Publ. 617, 1984, 445.
4. Saunders J. B., *J. Res. Natl. Bur. Stand.*, 1972, **76C**, 11-20.
5. Fujii K., Masui R., Seino S., *Metrologia*, 1990, **27**, 25-31.
6. Leistner A., Giardini W., *Metrologia*, 1991/92, **28**, 503-506.
7. Giacomo P., *Metrologia*, 1982, **18**, 33-40.
8. Davis R. S., *Metrologia*, 1992, **29**, 67-70.
9. Birch K. P., Downs M. J., *Metrologia*, 1993, **30**, 155-162.
10. Birch K. P., Downs M. J., *Metrologia*, 1994, **31**, 315-316.
11. Personal communication.
12. *Recommended Reference Materials for the Realisation of Physicochemical Properties* (Edited by K. N. Marsh), Oxford, Blackwell Scientific Publications, 1987, 14-15.
13. Kell G. S., *J. Chem. Eng. Data*, 1975, **20**, 97-105.
14. Thiesen M., Scheel K., Diesselholst H., *Wiss Abhandl. Physik. Tech. Reichs.*, 1900, **3**, 1-70.
15. Watanabe H., *Metrologia*, 1991, **28**, 33-43.
16. Takenaka M., Masui R., *Metrologia*, 1990, **27**, 165-171.
17. Bigg P. H., *Br. J. Appl. Phys.*, 1967, **18**, 521-525.
18. Kell G. S., *J. Phys. Chem. Ref. Data*, 1977, **6**, 1109-1131.
19. Chappuis P., *BIPM Trav. Mem.*, 1907, **13**, D1–D40.
20. Giardini W. J., Miles J. R., *CSIRO-DAP Technical Memorandum*, No. M12, Melbourne, CSIRO Division of Applied Physics, 1991.

Received on 27 October 1993 and in revised form on 3 August 1994.